© 2016 IJSRSET | Volume 2 | Issue 5 | Print ISSN: 2395-1990 | Online ISSN : 2394-4099
Themed Section: Engineering and Technology

Golden Section Search based Maximum Power Point Tracking Strategy for a Dual Output DC-DC Converter

Gayathri. R., K. Harish Reddy, Dr. Angeline Ezhilarasi

School of Electrical and Electronics Engineering, VIT University, Vellore, Tamil Nadu, India

ABSTRACT

This paper shows the analytical performance of maximum power point tracking for a photovoltaic system. In contemplation for photovoltaic (PV) systems to escalate their efficiency of power generation, it is mandatory to locate the Maximum power point (MPP) under all possible illumination conditions. The current-voltage (I-V) characteristics of PV devices are non-linear in nature, thereby the , MPP varies with changing elemental and environmental conditions. Maximum power point tracking (MPPT) control is expected to obtain the MPP irrespective of the device and climatic changes. This paper presents the implementation of Golden section search method for tracking the MPP. The algorithms are implemented using an Aurdino microcontroller ATMEGA328 and was tested for various operating conditions. In this system, a regular 250W solar panel was used for model interpretation, and results of simulation were correlated.

Keywords : Dual output, MPPT, GSS, PV

I. INTRODUCTION

In day to day life, there is an increase in the power density due to development of power electronics and material science. Renewable energy sources plays an crucial role to accommodate the power demand. Hence,it is essential to come up with inventive explications to cut down and preserve energy use[1]. Solar energy is one of the most significant source of energy. In the last two decades, photovoltaics (PV), also known as solar PV, has emerged from a small scope applications towards becoming a dominant electricity provenience [2]. The field of photovoltaic (PV) solar energy has accomplished a phenomenal rise for the past two decades in its outspread use from stand alone to utility interactive systems. The photovoltaic industries aims to build efficient and economical ystems that can be competitive with other energy sources. A PV system precisely converts sunlight into electricity. The main hindrance of PV systems include high device cost and low energy conversion efficiency. In order to lessen the price of energy, it is important to maintain the PV operation at its maximum efficiency at all time, and hence maximum power point tracking plays an crucial role.

Maximum power point tracking (MPPT) is an approach that charge controllers use for wind turbines and photovoltaic (PV) solar systems to maximize power output and many algorithms have been proposed to track the maximum power point in order to get better efficiency[11]. Maximum power point tracking(MPPT) control of the PV system intents to find out the MPP for online operation, irrespective of the shifts in the PV elemental and environment conditions. Many MPPT procedures have been suggested [5-10], these techniques differs by countless conditions, which encompass simplicity, convergence speed, hardware implementation, sensors, and the need for parametrization. Among these, perturb-and-observe(P-O), hillclimbing (HC),and incremental conductance (INC) are the most commonly used methods. Golden Section Search [12-13] and Perturb and Observe methods are the techniques to be used in this paper.

This paper is organized as follow:Section I, gives the system characterisation.Section II, gives the maximum power point algorithm techniques which was implemented on the proposed dual output non-inverting converter and Section III gives the simulated and

Section IV, the hardware results and at last section V, concludes the paper, followed by the references.

II. METHODS AND MATERIAL

1. System Description

The overall block diagram of the system is as shown below in the Figure.1. This system consists of an PV module interfaced with the load through an DC-DC Converter. The pulse to the converter is given through the maximum power point tracker. The characteristics of each block are explicated in the following sections.

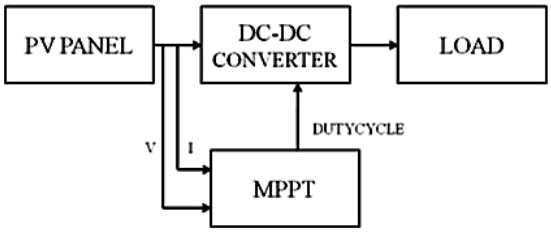

Figure 1. Block Diagram Of The Overall System

A. Modelling of Solar Cell

A solar cell is an electrical appliance that converts the energy of light directly into electricity by the photovoltaic effect. In other words, a solar cell is defined as a device whose electrical characteristics, such as current, voltage, or resistance, vary when disclosed to light. Solar cells are the building blocks of photovoltaic modules, otherwise known as solar panels. It can be represented in two ways namely, single diode model and two diode model. In this paper, we consider the single diode model [3].

The proportionate circuit of an single diode model of a solar cell is as given below in the figure 2.

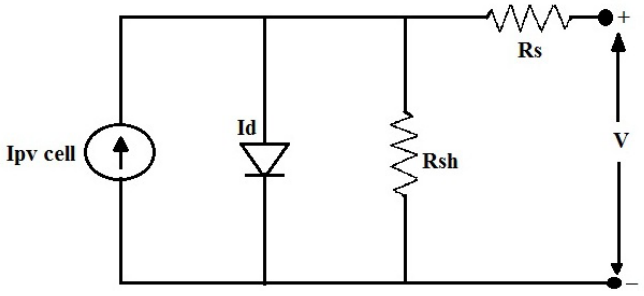

Figure 2. Equivalent Model Of an Solar Cell

Solar cells comprises of a p-n junction,fabricated in the layer of semiconductors, whose electrical characteristics diverges marginally from a diode, characterized by the equations given below. As shown in the figure, it comprises of an current source which is in parallel with the diode, wherein the output of the current source is directly reciprocal to the amount of light falling on the cell[4]. The modelling of the cell is as shown below:

$$I = I_{pvcell} - I_{diode} \quad (1)$$

Where,

Ipvcell is the current due to the incidence of light,
Idiode is the Shockley diode equation ,

The fundamental equation of the primary PV system given above does not produce the I-V characteristic of practical PV arrays. Practical modules consists of several connected PV cells that requires the inclusion of additional parameters such as Rs and Rp,which are as given below:

$$I = I_{pv} - I_o[exp(\frac{V + IR_s}{\alpha V_t}) - 1] - \frac{V + IR_s}{R_p} \quad (2)$$

The current due to the light produced by the module calculates linearly on solar irradiation and temperature, which is given by the following equation:

$$I_{pv} = (I_{pv,n} + \Delta T K_I)\frac{G}{G_n} \quad (3)$$

Where,
KI is the Temperature coefficient of short circuit current
G is the irradiance
Gn is the irradiance at standard operating conditions
q is the electron charge,
k is the Boltzmann constant
T is the product of actual and nominal Temperature of the p-n junction

The diode saturation current Io depends on temperature and can be expressed by the following equation:

$$I_o = I_{o,n}(\frac{T_n}{T})^3[exp[\frac{qE_g}{k\alpha}(\frac{1}{T_n} - \frac{1}{T})]] \quad (4)$$

Where,
Eg is band gap energy of semiconductor
Io;n is nominal saturation current
The final output current equation of a solar cell is as given below:

$$I_o = \frac{I_{sc,n} + K_I \Delta T}{e[V_{oc,n} + (\frac{K_v \Delta T}{V_t \alpha} - 1)]} \quad (5)$$

Where,
Voc;n is open circuit voltage,
Isc;n is short circuit current,
Vt is thermal voltage,
T is the temperature at standard operating conditions.

B. DC-DC converter Modelling

In this paper, a non-inverting dual output converter is proposed for interfacing the load with the panel. The proposed converter has three switches, three diodes and two inductors.

Two switches S2,S3comes under the low side switches and remaining S1is a high side switch. With the first two switches S1,S2 the boost gain is defined and with first S1 and last S3 switch the buck gain is defined. The diode D1 acts as a freewheeling diode. The Equivalent circuit diagram of the proposed converter is as shown below in the figure.3. The converter has two outputs. One acts as a boost output and the other buck output. Boost output can be taken as a DC link voltage and buck output is to charge a battery. The capacitors acts as voltage output filters. The proposed Converter has four modes of operation.

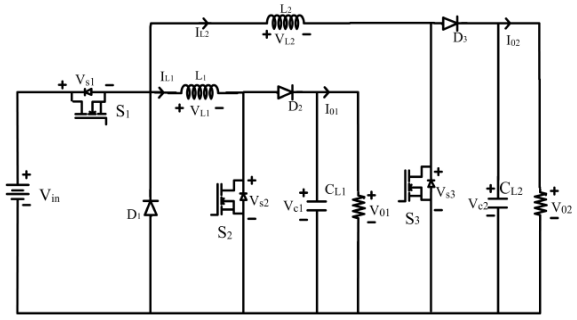

Figure 3. Dual Output DC-DC Converter

Mode 1. This mode of operation exists between times t0 and t1 as shown in Fig.4. In this mode, all the switches S1, S2, S3 are turned on. The inductors L1 and L2 start charging as shown in Figure.4. The inductor L1 charges via V in+, S1, L1, S2, and V in-. The inductor L2 charges from V in+, S1, L2, S3, and V in-. The charging paths in mode1 are shown in Figure. The diodes D1, D2, D3 are reversed biased. The capacitors CL1 and CL2 are stacked to discharge for the load R01, R02 respectively, and the duty cycle is represented by d.

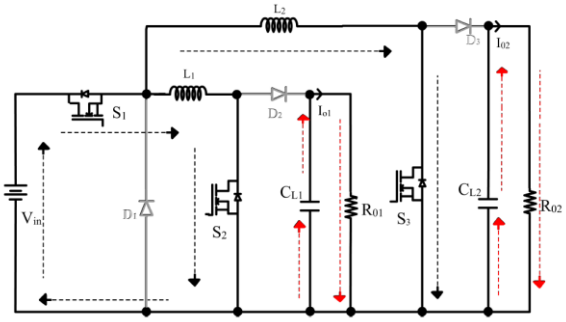

Figure 4. Operation of converter in mode 1

The KVL equation for L_1 path of charging is

$$-Vin + \frac{L \triangle I_1}{d_3 K} = 0 \tag{6}$$

$$d_3 K = \frac{L \triangle I_1}{Vin} \tag{7}$$

The KVL equation for L_2 is

$$-Vin + \frac{L \triangle I_2}{d_3 K} = 0 \tag{8}$$

$$d_3 K = \frac{L \triangle I_2}{Vin} \tag{9}$$

Mode 2. In this mode of operation from t1 to t2 switch S3 is turned off and the other switches S1, S2 remains in ON position. The diode D3 is forward biased. The energies of the stored inductor L2 and input voltage, are in series, thereby release their energies to load and capacitor CL2, meanwhile the inductor L1 remains in charging condition from the input voltage source. The charging and discharging path of inductors L2 and L2 are represented in Figure.5. The discharging path for inductor L2 is L2, load, Vin-. The turn on time of switch S3 is d3K and the period from S3 to S1 is (d1-d3)K, where d represents the duty cycle.

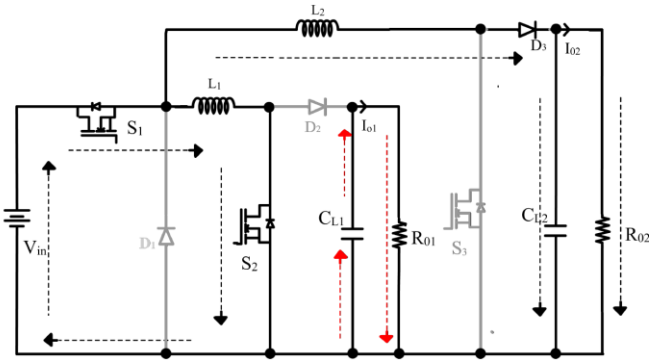

Figure 5. operation of converter in mode 2

The KCL is as obtained below

$$I_{L1} = I_{c1} + I_{o1} \tag{10}$$

$$-Vin + \frac{L \triangle I_1}{(d_1 - d_3)K} = 0 \tag{11}$$

$$(d_1 - d_3)K = \frac{L \triangle I_1}{Vin} \tag{12}$$

$$I_{L2} = I_{c2} + I_{o2} \tag{13}$$

$$-Vin + \frac{L \triangle I_2}{(d_1 - d_3)K} + V_{02} = 0 \tag{14}$$

$$(d_1 - d_3)K = \frac{L \triangle I_2}{Vin - V_{02}} \tag{15}$$

Mode 3. In this mode of operation from t_2 to t_3 the switches

S_1 and S_3 are turned off and switch S_2 is turned on. When the switch S_1 is turned off,the diode D_1 is forward biased. The current path of inductor L_1 L_2 is shown in Figure. 6. The stored energy in the capacitor is released to the load R_{01}. The inductor L_2 continues its discharge to the capacitor C_{L2} and to the load R_{02}.

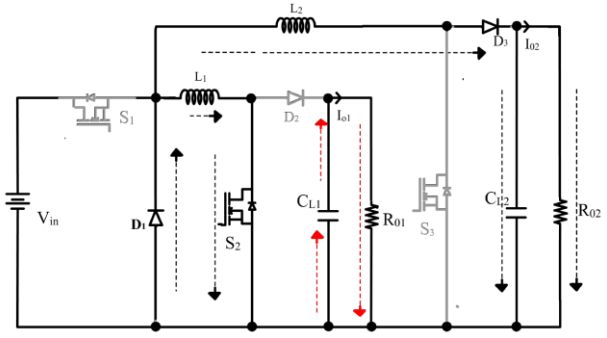

Figure 6. operation of converter in mode 3

The turn on time of switch S_2 is d_2K. The period from S_1 to S_2 is $(d_2 - d_1)K$.

$$-\frac{L \triangle I_2}{(d_2 - d_1)K} + V_{02} = 0 \tag{16}$$

$$(d_2 - d_1)K = \frac{L \triangle I_2}{V_{02}} \tag{17}$$

Mode 4. This mode operates from t_3 to t_4 and all the switches S_1, S_2, S_3 are turned off and energies stored in the inductors are released to the capacitors and to the respective loads. The discharge path of the inductor L_1 is L_1, D_2, R_{01}, D_1 and for the inductor $L_2$is L_2, D_3, R_{02}, D_1. The diodes D_1, D_2, D_3 are forward biased. The current path is shown below in the Figure.7

$$-\frac{L \triangle I_1}{(1 - d_2)K} + V_{01} = 0 \tag{18}$$

$$(1 - d_2)K = \frac{L \triangle I_1}{V_{01}} \tag{19}$$

$$\frac{L \triangle I_2}{(1 - d_2)K} + V_{02} = 0 \tag{20}$$

$$(1 - d_2)K = \frac{L \triangle I_2}{V_{02}} \tag{21}$$

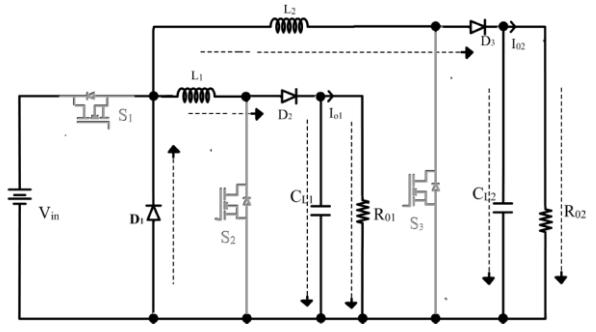

Figure 7. operation of converter in mode 4

From the typical waveform from equations 7; 12; 16, the gain of the converter for boost mode is

$$V_{02} = \frac{V_{in} d_1}{(1 - d_3)} \tag{23}$$

The gain can be calculated using the equations 4; 9; 11; 15.

The gain of the converter in the buck mode is

$$T = d_3 + (d_1 - d_3) + (d_2 - d_1) + (1 - d_2)K \tag{24}$$

The critical inductance for boost mode is calculated

$$L_1 = \frac{R_{01}(1 - d_2)}{2f(2d_1 + 1 - d_2)} \tag{25}$$

Where d_1, d_2, d_3 are the timing intervals between modes of operation. From equations 7; 12; 16 the critical inductance is given for Inductance L_1

$$L_2 = \frac{R_{02}}{2f(\frac{d_1}{1-d_3} + \frac{d_1}{1-d_3-d_1}) + 2} \tag{26}$$

From the equations 9; 14; 16; 19, the critical inductance is given for Inductance L_2

2. Maximum Power Point Tracking Algorithms

Maximum power point tracking (MPPT) is an approach used by charge controllers for wind turbines and PV solar systems to maximize power output[5]. PV solar systems occurs in several configurations.Solar cells have a convoluted link between temperature and total resistance that gives a non-linear output efficiency which can be evaluated based on the I-V curve. It is the objective of the MPPT system to fragment the output of the PV cells and employ proper resistance (load)in order to obtain the maximum power for any given environmental conditions. MPPT devices are commonly integrated into an electric power converter system that provides voltage or current conversion, filtering, and regulation for driving various loads, including power grids, batteries, or motors[6]. MPP amounts to the product of MPP voltage(Vmpp) and MPP current(Impp).Given below, are the two MPPT techniques, that are used in this paper for analysis.

A. Perturb and Observe Method

In this method, the controller modifies the voltage by a small amount from the array and calculates power; if the power increases, further changes in that direction are tried until power no longer increases. This is called the perturb and observe method and is most common, although this method results in oscillations of power output.[5-6] It is referred, to as a hill climbing method, because it depends on the rise of the curve of power against voltage below the maximum power point, and

the fall above that point.[7].The Flowchart that depicts the algorithm is as given in the Figure.8. Perturb and observe is the most commonly used MPPT method due to its ease of implementation.[5] Perturb and observe method may result in top-level efficiency, provided that a proper predictive and adaptive hill climbing strategy is adopted[14].

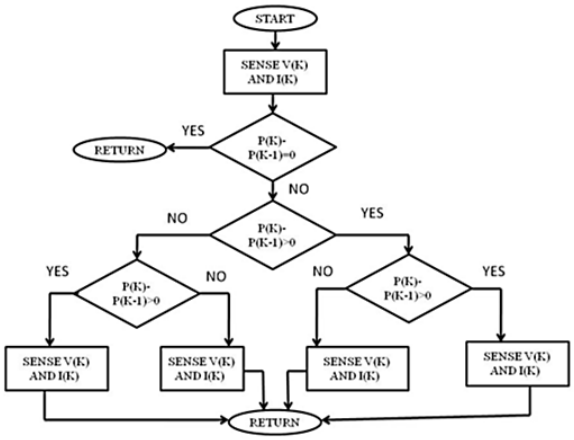

Figure 8. Flow Chart of The Algorithm

Although Perturb and Observe method is widely used, it has major disadvantages which are as given below. If there is any shadow on any of the panels (because they have been in series or parallel) then the power- voltage curve of the PV will have several peak and Perturb and Observe method can't find the real peak[9]. One of the major prejudice, of perturb and observe method is that based on the algorithm, the system will continue to oscillate around the maximum power point. This can lead to inefficiencies, especially in situations when the irradiance is low and the power-voltage curve begins to flatten out. When this occurs, the perturb and observe method can sometimes have difficulty determining when it has actually reached the maximum power point. In addition, sometimes, this algorithm will perform several iterations in the wrongdirection if it is affected by rapidly changing conditions [15].

Thus, in order to overcome these disadvantages we go for another iteration-based algorithm which is as given in the next section.

B. Golden Section Search method

The golden section search is a technique that is used for discovering the minimum or maximum of a strictly uni-modal function by individually narrowing the range of values inside which the extremum is known to exist[12]. This method is vigorous and also has a faster feedback compared to the other traditional algorithms. The algorithm was simulated and verified.

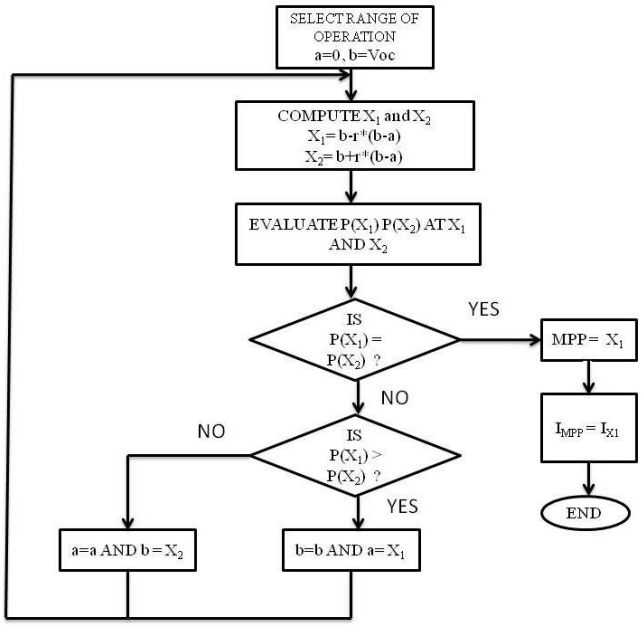

Figure 9. Flow Chart of the Algorithm

The main aim is to find maximum functional value within the input interval [a,b]. Two points are selected in the interval [a.b] and the function is evaluated at these points. Points are selected in such a way that each point subdivides the interval into two parts and length of whole line/length of larger fraction = length of larger fraction/length of smaller fraction. Assume a line segment as shown in the figure.10 It gives from 0 to voc. The length from b to X1 is given by r and the length from X2 is given by 1- r.The values are calculated using the formulas given in the flowchart above, and the corresponding powers are calculated at these points and the rest of operation is as illustrated in the flowchart. For a GSS based MPPT for photovoltaic system, the PV characteristics are the operating characteristics wherein the main function corresponds to power, whose maximum value has to be captured. The spectrum of operation is from zero to open circuit voltage (Voc); that is, a = 0, b = Voc with r = 0.618. [13]

The way of tracking maximum point is shown in the Figure.9. The voltage corresponding to the maximum power is obtained and mapped into the V-I characteristics to achieve the current reference.

C. GSS with voltage as search parameter

The detailed GSS algorithm at standard operating conditions that is, G= 1000 W=m2 and temperature at 25_C and with an open circuit voltage of 30V is as given below in the table. I

III. RESULTS AND DISCUSSION

A. PV Module Simulation

The PV Module Simulation is done in MATLAB. The simulation is done at standard conditions in order to check the MATLAB model PV Panel. The Input to the panel is given es based Energy consumption

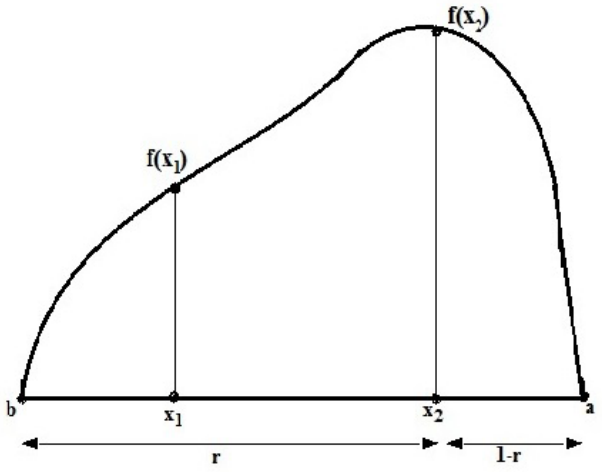

(a) MPPT tracking with GSS algorithm

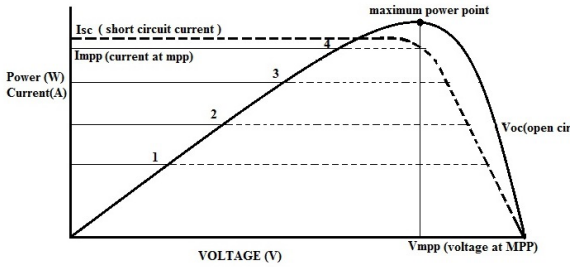

(b) Division of Intervals

Figure 10. GSS algorithm

TABLE I. SEARCH ALGORITHM AT STANDARD OPERATING CONDIDTIONS

STEP	a	b	x_1	x_2	P_1	P_2	COMMENT
1	0	30	13	20	98	155	$P_2 > P_1$
2	13	29.9	21	25	163	192	$P_2 > P_1$
3	21	32.9	25	28	192	199	$P_2 > P_1$
4	25	32.9	28	30	199	176	$P_1 > P_2$
5	25	30	26	28	200	199	$P_1 > P_2$
6	25	28	26	27	197	200	$P_2 > P_1$
7	26	28	27	27	200	200	$P_1 = P_2$

According to the data-sheet of the panel used which is given in the table. The unknown parameters are evaluated and power voltage and current-voltage characteristics are simulated. The unknown parameters, saturation current at reference temperature Ior, saturation current Io and Short circuit current Isc at the given temperature are calculated from the input parameters which is given in the table.II

TABLE II. PARAMETERS OF PANEL AT STANDARD CONDITIONS

S.NO	PARAMETERS	VALUE
1	Peak Power	250W
2	Maximum Voltage	35.80V
3	Maximum Current	8.30A
4	Output Voltage	200V
5	Output Current	1.2A

In this paper, ELDORA VSP.60.AAA.03 silver series/ Polycrystaline solar PV modules are used. The table. II shows its electrical specifications from the datasheet. In this PV module, 60 cells are connected in series-parallel combina tion.All the technical datas are taken at standard test condition, that is, at an standard irradiance level of 1000 W=m2 and at an temperature T = 25C. The table.III gives the simulated output and input parameters to the panel.The unknown parameters are saturation current at reference temperature Ior, saturation current Io and Short circuit current Isc at the given temperature are calculated from the input parameters.

TABLE III. SIMULATED VALUES

S.NO	PARAMETERS	SIMULATED VALUE
1	Input voltage	30V
2	Input current	8.27A
3	Input power	248W
4	Reverse saturation current	2.623 ×(10e-7)
5	Saturation current	2.623 ×(10e-7)
6	Short circuit current	8.2A
7	Maximum power point	200W
8	Voltage at maximum power point	26V

1) Variation of IV and PV curve at Different irradiation : In

order to verify the model under different operating conditions, several tests have been performed at various temperature and solar irradiance values. The figure below shows the IV curves and PV curves for various solar irradiance G varies from 600 W=m2 to 1000 W=m2 at standard cell temperature of 25oC. The IV curves at varying operating conditions are as shown in the Figure 12. The irradiance is varied for three cycles

with a constant temperature and the curves are recorded.

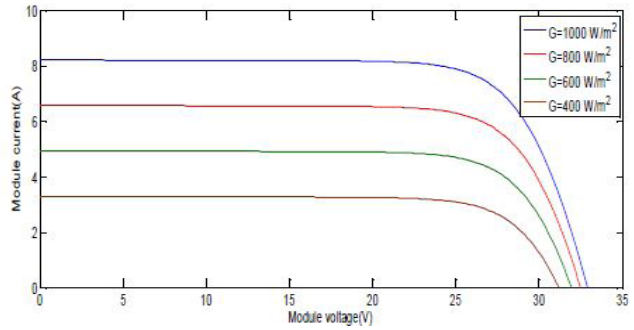

(a) IV curves at different irradiation and constant temperature

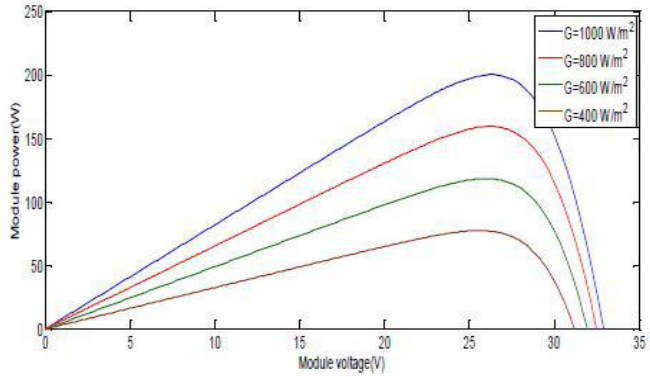

(b) PV curves at different irradiation and constant temperature

Figure 11. CURVES AT DIFFERENT OPERATING CONDITIONS

From the curves it is seen that, PV curve has negligible effect on the open circuit voltage ,due to the variation of irradiation and mainly affects short circuit current. 2) Variation of IV and PV curve at Different temperature : The IV characteristics with constant radiation and different temperature are shown in Figure.13. It is seen from the curve that IV curve has negligible effect on the short circuit current due to the variation of temperature and mainly affects open circuit voltage.

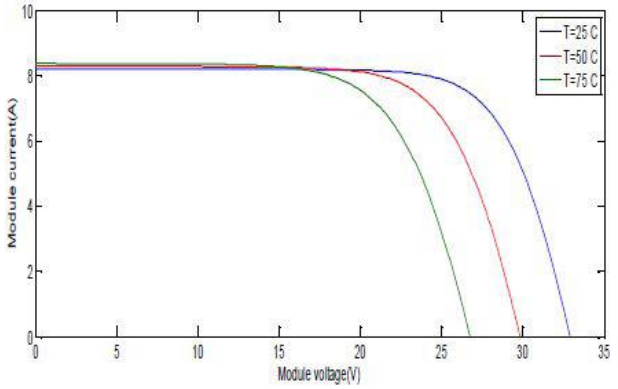

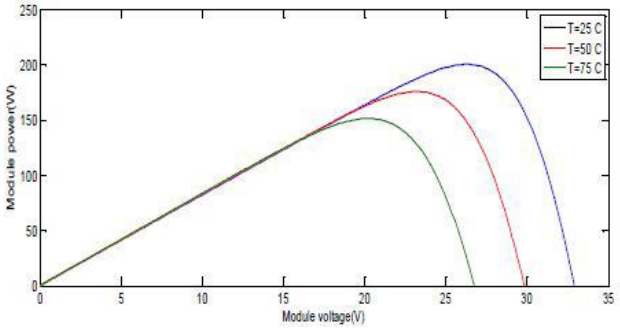

Figure 12. IV curves at different temperature and constant irradiation

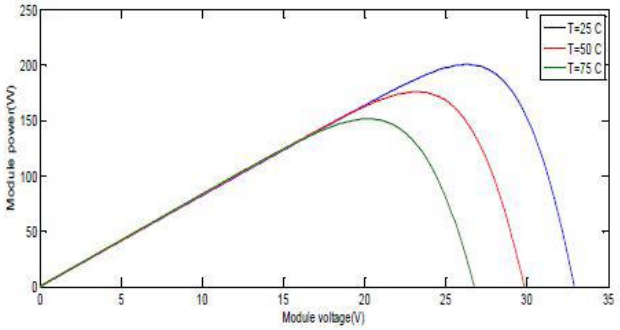

Figure 13. PV curves at different temperature and constant irradiation

B. Maximum Power Point Tracking Simulation

The algorithms were tested at various irradiation conditions and the value was recorded. The table.IV shows the variation of duty cycle for different irradiation conditions.

TABLE IV. DUTY CYCLE FOR DIFFERENT IRRADIATIONS

S.NO	IRRADIANCE	V_{in}	I_{in}	DUTYCYCLE	V_{out}	I_{out}
1	600	25	8.20	0.25	48	4.2
2	800	28	8.23	0.37	52	4.4
3	1000	30	8.29	0.5	59	4.3

The duty cycle obtained from the maximum power point block in order to drive the switch is as shown in the Figure.15. It gives the variation of duty cycle at various operating conditions.

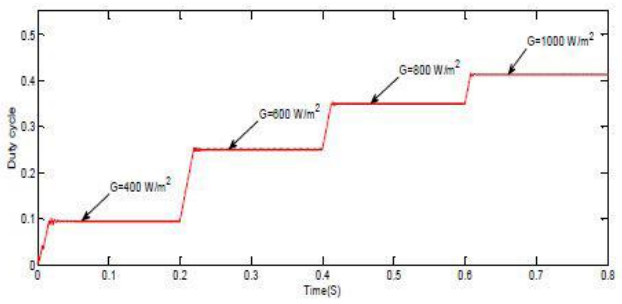

Figure 14. Duty cycle with constant temperature and different radiation

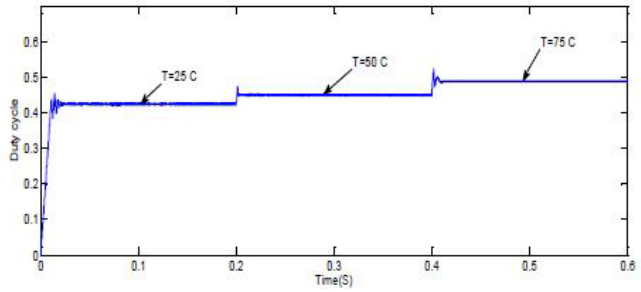

Figure 15. Duty Cycle with constant radiation and different temperature

The system is tested for both open loop i.e without MPPT and closed loop i.e with MPPT, Readings for both the conditions was taken with intervals of time for whole day. Readings were tabulated and the impedance curve was plotted which is as shown in the Figure 16.

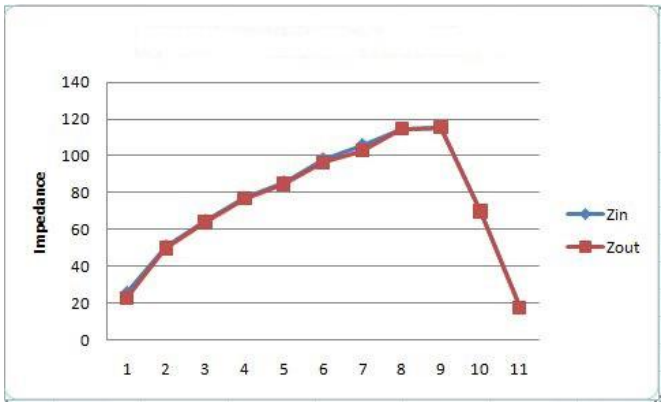

Figure 16. Impedance curve with MPPT

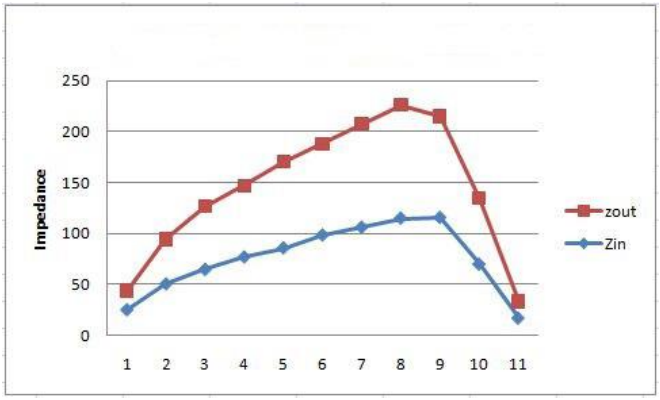

Figure 17. Impedance curve without MPPT

From the Graph (b) it is seen that,impedance of load and source will be different as there is no MPPT,hence only partial transfer of power occurs, whereas, Graph (a) gives the impedance curve while using MPPT. From the graph it is interpreted that the MPPT algorithm matches the load impedance with the source impedance, which is the condition for maximum power transfer.

C. Comparison of algorithms

The table.V below gives the comparison of both the algorithms for various parameters:

TABLE V. MAJOR CHARACTERISTICS COMPARISON OF ALGORITHMS

TECHNIQUE	CONVERGENCE	PARAMETERS	COMPLEXITY
Perturb And Observe	Medium	V,I	Medium
GSS	Fast	V,I	Low

D. Hardware Results

The hardware setup of PV standalone system with PV module is tested at 240 W power with a frequency of 72KHz. The DC-DC converter, Arduino Uno board ATMEGA328, MOSFET driver circuit and power supply unit are integrated . Voltage and current sensors are used in order to sense the respective voltage and current from the panel.The table.VI below gives the designed electrical specifications of the converter. The whole setup was analysed and the maximum power point algorithms were implemented using ATMEGA328 . The duty cycle obtained is as shown in the Figure.20 at standard operating conditions. The power circuit is as given below in the Figure.18

TABLE VI. DESIGNED ELECTRICAL SPECIFICATIONS

PARAMETERS	DESIGNED VALUES
L_1	570 μH
L_2	220 μH
C_{L1}	47 μF
C_{L2}	47 μF
R_{01}	570 Ω
R_{02}	23.6 Ω

PARAMETERS DESIGNED VALUES
L1 570 _H
L2 220 _H
CL1 47 _F
CL2 47 _F
R01 570

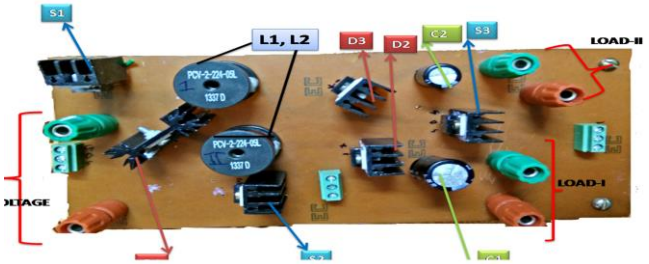

Figure 18. Power Circuit

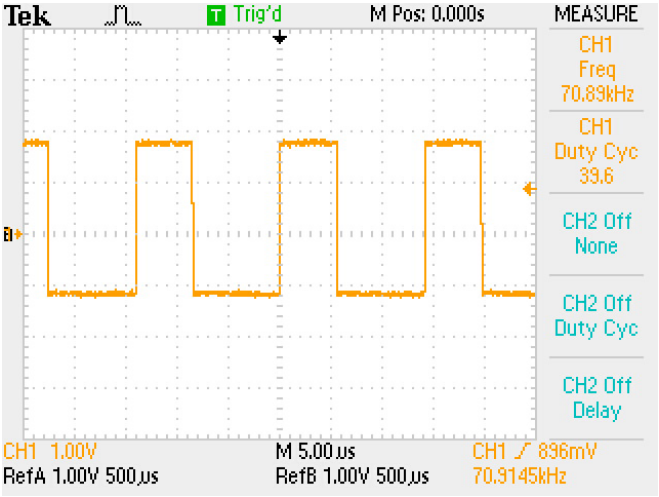

Figure 19. duty cycle

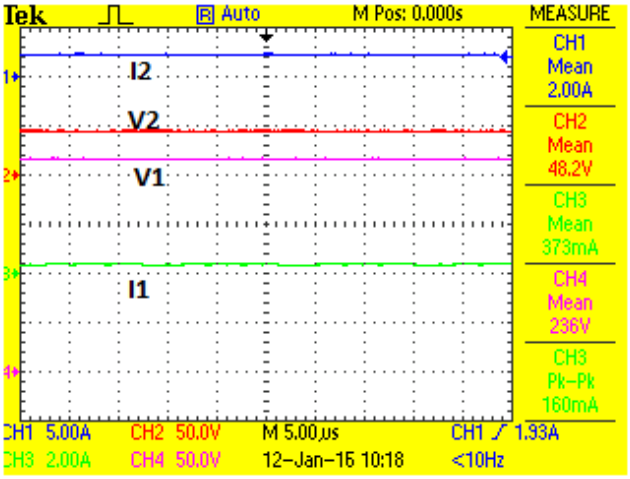

Figure 20. output at standard operating conditions

The output parameters are as obtained above. The boost output voltage around 240 V and boost current 373mA, along with buck output voltage 48 V with buck current 2.0 A is obtained. The gain of the converter is as obtained below, when the duty cycle from the maximum power point tracker varies.

They are plotted as shown below in the Figure.21.From the graph it is seen that, when the duty cycle to the converter increases, the gain also increases which implies that they are in proportion.

IV. CONCLUSION

In this work, it is found that the current-voltage relationship is non linear and there is a maximum power at a peculiar current and voltage. This maximum power is varying with regard to the atmospheric conditions such as irradiation value of solar light, atmospheric temperature and shading etc. In this paper, evaluation with regard to the changes in the effect of irradiation and atmospheric temperature on current – voltage characteristics and power - voltage characteristics are studied.

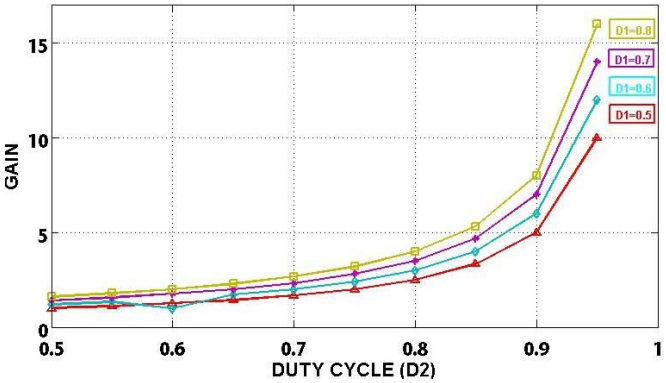

Figure. 21. Voltage Gains of the converter

When the irradiation level decreases, the photo generated current goes down significantly. The open circuit voltage (Voc) also drops, but the effect is negligible. In decreasing atmospheric temperature value, at solar irradiation of 1000 W=m2 ,open circuit voltage is only decreased and the photo generated current remain constant. The performance of the MPPT with GSS based algorithm indicates good agreement with the simulated results. The s teady state performance of the converter shows the balance voltage operation.This indicates the converter performance with its efficiency up to 84 is achieved, in these converters with high voltage gains in the PV energy conversion systems.

V. REFERENCES

[1] Wikipedia. Renewable energy database. Available at http://www.en.wikipedia.org/wiki/Renewable energy Growth of renewables, accessed February

[2] Bucciarelli, L.L., Grossman, B.L., Lyon, E.F., et al. The energy balance associated with the use of a MPPT in a 100 kW peak power system. Proc.

IEEE Photo voltaic Specialist Conf. (PVSC), 1980, pp. 523527"

[3] Model of photovoltaic Module in Matlab,Francisco M. Gonzlez- Longatt,(II CIBELEC 2005).

[4] Modeling of photovoltaic module, International Conference on Renewable Energies and Power Quality"(ICREPQ10) Granada (Spain), 23th to 25th March, 2010.,Ramos Hernanz, JA. Campayo Martin,JJ. Zamora Belver,I., Larranga Lesaka,J. , Zulueta Guerrero,E. p

[5] Comparison of Photovoltaic Array Maximum Power Point Tracking Techniques", T.Esram and P. L.Chapman,IEEE Transactions on Energy Conversion, Vol. 22, No. 2, 2007.

[6] T.Esram and P. L.Chapman, "Comparison of Photovoltaic Array Maximum Power Point Tracking Techniques," IEEE Transactions on Energy Conversion, Vol. 22, No. 2, 2007

[7] E.I.O. Rivera, "Maximum Power Point Tracking using the Optimal Duty Ratio for DC-DC Converters and Load Matching in Photovoltaic Applications," Twenty Third Annual IEEE Applied Power Electronics Conference and Exposition, APEC 2008, pp. 987-991, 2008.

[8] D.Peftsis, G. Adamidis, P. Bakas and A. Balouktsis, "Photovoltaic System MPPT Tracker Implementation using DSP engine and buckboost DC-DC converter", 13th Power Electronics and Motion Control Conference, 2008."

[9] D.P.Hohm and M. E. Ropp, Comparative Study of Maximum Power Point 1Tracking Algorithms Using an Experimental, Programmable, Maximum Power Point Tracking Test Bed, IEEE Proc. Of photovoltaic specialists conference, pp. 1699-1702, 2000.

[10] L.Nguyen, Modeling and Simulation of Solar PV Arrays under Changing Illumination Conditions, In Proc. IEEE Workshops on Computer in Power Electronics, ,pp. 866-870, 16-19 July 2005.

[11] Johan H. R. Enslin, Mario S. Wolf, Daniel B. Snyman, and Wernher Swiegers, Integrated Photovoltaic Maximum Power Point Tracking Converter, IEEE Trans., Vol. 44,no.6, pp. 1036-1047, Aug .2009.

[12] R. Shao and L. Chang, A new maximum power point tracking method for photovoltaic arrays using golden section search algorithm, in Proceedings 1of the IEEE Canadian Conference on Electrical and Computer Engineering (CCECE 08), pp. 619622, May 2008.

[13] J. Agrawal and M. Aware, Golden section search (GSS) algorithm for maximum power point tracking in photovoltaic system, in Proceedings of the IEEE 5th India International Conference on Power Electronics (IICPE 12), 6, p. 1, Delhi, India, December 2012. 14Maximum Power Point Tracking Scheme for PV Systems Operating Under

[14] Partially Shaded Conditions Hiren Patel and Vivek Agarwal, Senior Member, IEEE TRANSACTIONS ON INDUSTRIAL ELECTRONICS, VOL. 55, NO. 4, APRIL 2008"

[15] A Hardware Implementation and Analysis of Testing MPPT Algorithmson PV Modules,Derryn Harvie,Dr.Sumedha Rajakaruna, Australasian Universities Power Engineering Conference, AUPEC 2014, Curtin University, Perth, Australia, 28 September 1 October 2014"